A Journal of the Gesellschaft Deutscher Chemiker
Angewandte Chemie
GDCh
International Edition
www.angewandte.org

Title: Synergistic Covalent and Supramolecular Polymers for Mechanically Robust yet Dynamic Materials

Authors: Zhaoming Zhang, Lin Cheng, Jun Zhao, Lei Wang, Kai Liu, Wei Yu, and Xuzhou Yan

To be cited as: *Angew. Chem. Int. Ed.* 10.1002/anie.202004152

Link to VoR: https://doi.org/10.1002/anie.202004152

WILEY-VCH

Synergistic Covalent and Supramolecular Polymers for Mechanically Robust yet Dynamic Materials

Zhaoming Zhang,[a] Lin Cheng,[a] Jun Zhao,[a] Lei Wang,[a] Kai Liu,[a] Wei Yu,[a] and Xuzhou Yan*[a]

[a] Dr. Z. Zhang, L. Cheng, J. Zhao, L. Wang, Dr. K. Liu, Prof. W. Yu, and Prof. X. Yan
School of Chemistry and Chemical Engineering, Frontiers Science Center for Transformative Molecules,
Shanghai Jiao Tong University, Shanghai 200240, P. R. China
E-mail: xzyan@sjtu.edu.cn

Supporting information for this article is given via a link at the end of the document.

Abstract: Nature has engineered delicate synergistic covalent and supramolecular polymers (CSPs) to achieve advanced life activities like the role of thin filament in muscle contraction. Constructing artificial synergistic CSP materials with bioinspired mechanically adaptive features, however, represents a challenging goal. Here, we report an artificial CSP system to illustrate the integration of covalent polymer (CP) and supramolecular polymer (SP) in a synergistic fashion, along with the emergence of notable mechanical and dynamic properties which are unattainable when the two polymers are formed individually. The synergistic effect relies on the peculiar network structures consisted of SPs and CPs, and thus makes the resultant CSPs an overall improvement in the mechanical performance of stiffness, strength, stretchability, toughness, and elastic recovery. Moreover, the dynamic properties including self-healing, stimuli-responsiveness, and reprocessing are retained in CSPs as well, manifesting themselves as programmable and tunable materials.

Introduction

Polymers are basic yet crucial components for living things due to their roles in constructing structural materials and participating in life process. These polymers are not only the well-known covalent polymers (CPs) but also a large variety of sophisticated supramolecular polymers (SPs). In fact, the implement of some complex functions in organisms relies on the polymers in a special form, namely, synergistic covalent and supramolecular polymers (CSPs). For example, in thin filament, tropomyosin as a CP binds to the SP of actin filament through noncovalent bonds to construct a synergistic CSP, which plays an important role in muscle contraction.[1] Mimicking nature is always an effective way to develop new materials.[2] Although it can be expected that synergistic CSPs would possess advanced properties that are unable to achieve by individual CPs or SPs, materials based on synergistic CSPs are really rare. In 2016, one ingenious system of simultaneous covalent and noncovalent hybrid polymerizations was reported by Stupp and coworkers, in which higher molecular weight covalent polymers were obtained compared to the polymers generated by the same polymerization without the synergy of a supramolecular polymer.[3] Similarly, other reported polymeric systems with coexisted SPs and CPs were also focused on the study of concurrent covalent and supramolecular polymerizations.[4] However, synergistic CSPs designed for specific properties or functions like thin filament have yet to be demonstrated.

CPs, the traditional sense of polymers, possess good robustness and strength but lack of dynamic properties. On the contrary, SPs have extraordinary performances in stimuli-responsive, self-healing, and self-adapting properties,[5] whereas the excellent dynamic properties are also accompanied by relatively poor mechanical properties. Owing to these inherent characteristics of CPs and SPs, developing polymeric materials in which good mechanical performance coexists with dynamic behaviors is always a significant challenge. Taking inspiration from bio-system, we speculate that construction of synergistic CSPs is able to achieve the goal, because intelligent integration of judiciously designed CPs and SPs in CSPs could combine their merits, and the synergistic effect in CSPs would further improve these merits or even create evolved properties.

Herein, we report a *de novo* chemical design of synergistic CSPs which simultaneously possess robust yet dynamic characteristics in a programmable manner. The key principle to the design is that the CSPs adopt network structures formed by the combination of SPs and CPs, which favors the synergistic effect to improve the mechanically adaptive properties. In the networks, the CPs serve as skeleton and maintain the integrity of the materials, and the SPs are able to undergo energy dissipation under external forces and thus tune the mechanical behaviors through the reversible dissociation and reassociation of the host−guest recognition. When they work synergistically, the mechanical performances of CSPs are much better than the simple sum of the corresponding properties of SPs and CPs. The improvements of the mechanical properties are comprehensive, including stiffness, strength, toughness, stretchability, and elastic recovery, which are also tunable by controlling the host−guest complexation in CSPs. Along with the dynamic properties of self-healing, stimuli-responsiveness, and reprocessing inherited from SPs, the CSPs, therefore, possess not only remarkable mechanical adaptabilities but also multiple dynamic properties.

Results and Discussion

Design, synthesis, and structural characterization. Polynorbornenes (PNBs) have attracted much research attention due to their great stability and easy preparation by ring opening metathesis polymerization (ROMP) of norbornene derivatives.[6] Host−guest molecular recognition between benzo-21-crown-7 (B21C7) and its complementary secondary dialkylammonium salt has been widely used to construct functional SPs owning to their

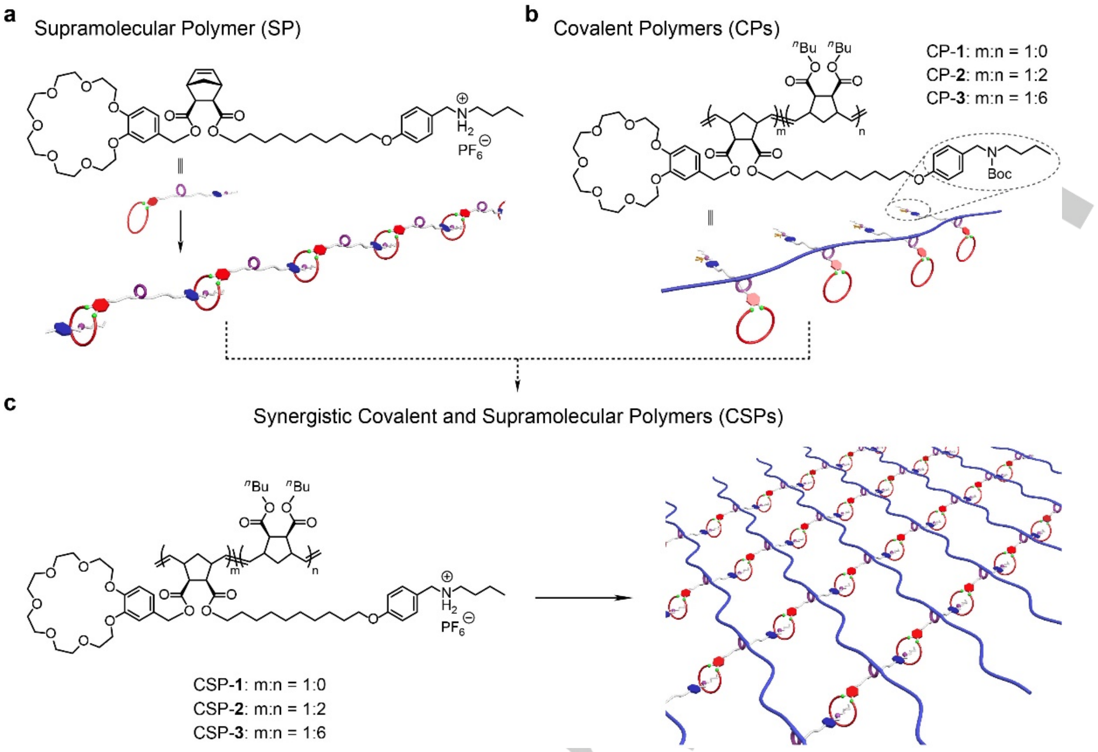

Scheme 1. a) Chemical structure and schematic representation of SP. b) Chemical structures and schematic representation of CPs. Boc-protected amino groups cannot be recognized by the crown ethers. c) Chemical structures and schematic representation of CSPs in which the inherent characteristics of SPs and CPs and their synergistic effect endow the CSPs with remarkable mechanical and dynamic properties.

moderate association constant (K_a = 250 M^{-1} in CH_3CN).[7] Therefore, we selected PNB as the covalent backbone and SP based on B21C7/secondary ammonium salt recognition motif as the noncovalent counterpart to construct synergistic CSPs. As shown in Scheme 1c, the PNB and SP chains interweave with each other through the node of the cyclopentane moiety, forming the synergistic CSP network structures. In fact, the network structures of CSPs can also be understood in two simple ways: on the one hand, CSPs-**1**–**3** can be seen as the CP chains strung together by SPs; on the other hand, the CSPs can be considered as the SP chains linked together by CPs as well. Obviously, the structures of synergistic CSPs are different from those reported systems in which the supramolecular interactions only serve as discrete crosslinks of CPs.[8] Notably, there would be some defects in the CSP networks due to the formation of cyclic oligomers during the supramolecular polymerization. But the linear supramolecular polymers are able to be predominant in bulk according to the ring-chain supramolecular polymerization mechanism (Scheme S1).[7c] With different amounts of SPs in the system, synergistic CSPs-**1**–**3** have been constructed. To make comparison, individual SP and CPs were also prepared as shown in Scheme 1a and 1b, respectively. The self-assembly of B21C7 and secondary ammonium salt units-decorated norbornene derivative forms the SP, which is nearly the same as the SP part extracted from the CSPs. As for the CPs, their structures are very similar to the CSPs except that the amino group was protected by the Boc rather than in the form of secondary ammonium salt, which is unfavorable for the host–guest recognition. It is worth noting that the CPs are also the starting materials to prepare CSPs, hence the molecular weight and structural composition of CSPs are very close to the corresponding CPs.

The formation of SP was supported by the ^1H NMR (Figure 1b). Compared with the spectrum of Boc-protected monomer **1** (Figure 1a and Scheme S2), the aromatic protons of supramolecular monomer showed both the complexed and uncomplexed peaks which can be attributed to the slow-exchange nature of the recognition motifs on the proton NMR timescale. Meanwhile, the characteristic peaks of crown ether (H_1–H_5) exhibited obvious downfield shift, which also supported the formation of the host–guest complexes. The detailed process of supramolecular polymerization in solution was tracked by concentration-dependent ^1H NMR and 2D diffusion-ordered NMR spectroscopies (Figures S25 and S26).

The syntheses of CPs-**1**–**3** were based on two monomers: as shown in Scheme S2, the monomer **1** is a norborene derivative containing substituents of B21C7 and Boc-protected amino group, and the monomer **2** is norbornenyl *exo*-di-*n*-butylester which acts as a diluent to tune the content of SPs in the final CSPs. Initiated by the third-generation Grubbs catalyst, the homopolymerization of monomer **1** produced the CP-**1**, and the random copolymerization of monomers **1** and **2** with the feed ratios of 1:2 and 1:6 afforded copolymers CP-**2** and CP-**3**, respectively. Taking CP-**3** as an example, the H_{10} signal of monomer **1**, the characteristic peak of double bond in norbornene moiety, disappeared after polymerization in the ^1H NMR spectra (Figure 1d). At the same time, broader signals emerged at 5.54 and 5.34 ppm could be ascribed to the *trans* and *cis* double bonds in the polymers.[9] The integration of the ^1H NMR spectra revealed that the ratios of the two repeating units corresponding to monomers **1** and **2** in the copolymers are roughly consistent with the feed ratios of the two monomers. Benefitting from controlling the ratios of the monomers/catalyst, the number-average molecular weights

10.1002/anie.202004152

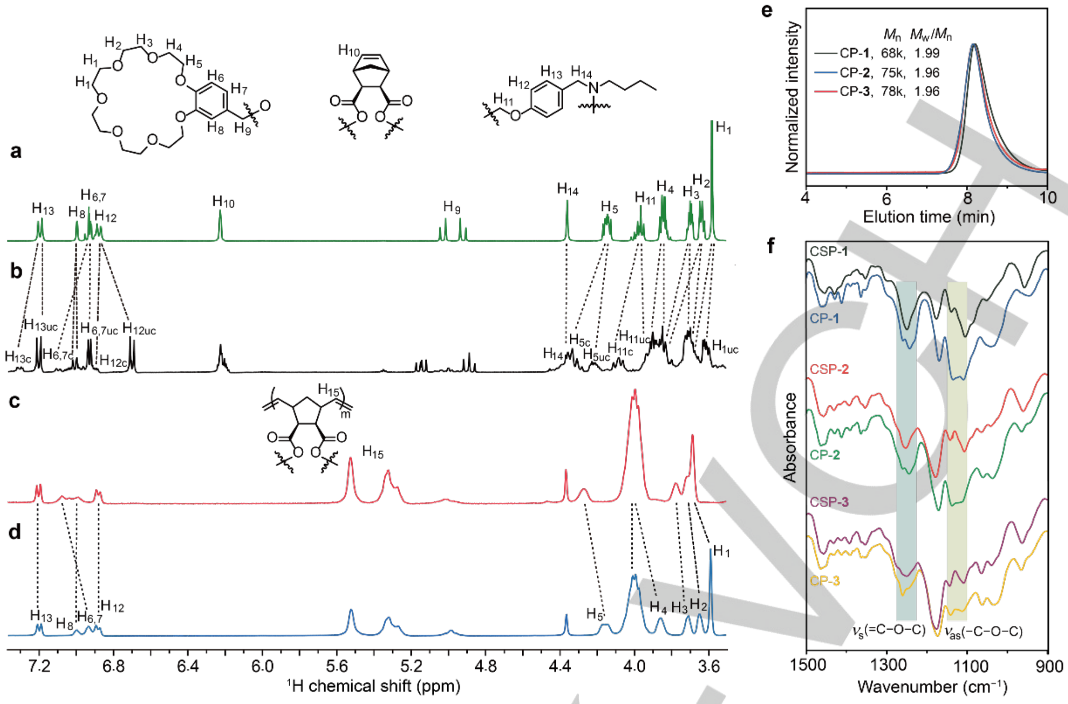

Figure 1. Partial ^{1}H NMR spectra (400 MHz, acetone-d_6, r.t.) of monomer **1** (a), SP (b), CSP-**3** (c), and CP-**3** (d). e) GPC elution curves of CPs-**1**–**3** with DMF as the eluent and PS as the standard. f) ATR-FT-IR spectra of CSPs-**1**–**3** and comparison with those of corresponding CPs-**1**–**3**.

(M_n) of the CPs-**1**–**3** measured by size exclusion chromatograph (SEC) were basically close to each other with the values of 68, 75, and 78 kDa, respectively (Figure 1e).

Based on CPs, the preparations of CSPs were readily realized by converting the *N*-Boc group into secondary ammonium salt: the *N*-Boc group was firstly deprotected by CF_3COOH, and followed by a treatment of NH_4PF_6 to exchange the counter anion into PF_6^-. In the ^{1}H NMR spectrum, the H_1–H_5 signals of B21C7 moiety in CSP-**3** shifted downfield compared with those of CP-**3**, which was caused by the recognition of B21C7 to secondary ammonium salt to form SP (Figure 1c and 1d). Thus, both the CP and SP were present in the system, indicating the formation of the CSP. So far, the synergistic CSPs in solution have been demonstrated, then the CSPs in the condensed state were investigated by FT-IR spectroscopy with attenuated total reflection (ATR) mode. As shown in Figure 1f, the peaks around 1140 cm^{-1} assigned as the ν_s (−C−O−C) of the B21C7 moiety shifted slightly to the lower frequency area when compared with those of the CPs, which was also observed in the similar case.[10] Besides, the changes of ν_{as} (=C−O−C) in B21C7 moiety at 1255 cm^{-1} also supported the formation of the host–guest complex.

Thermal properties of SP, CPs, and CSPs. In the thermal gravimetric analysis (TGA) curves of CSPs as well as CPs and SP, the decomposition temperatures of all these polymers were higher than 200 °C, exhibiting good thermal stabilities (Figure S27). Differential scanning calorimetry (DSC) curves can reveal some structure information of the synergistic CSPs. As shown in Figure 2a, the glass transition temperature (T_g) values of SP and CP-**3** were 14 and –22 °C, respectively. When the SPs were attached on the CPs to form CSPs, the T_g enhanced significantly. The values showed a trend of CP-**3** < CSP-**3** < CSP-**2** < CSP-**1**. This can be explained that in the synergistic CSPs, the CP and SP chains interweave with each other to form network structures, which can restrict the movements of CP chain segments. Furthermore, the more SPs were involved, the denser networks would be formed, hence leading to higher T_g.

Mechanical properties of SP, CPs, and CSPs. To study the effect of SP ratios on the mechanical properties, the tensile tests of CSPs-**1**–**3** were performed. The stress-strain curves and the calculated Young's modulus and toughness were shown in Figure 2b and 2c, respectively. The Young's moduli of CSPs-**1**–**3** decreased gradually from 285 to 216 and then to 92 MPa. On the contrary, the strain at break values were 3% for CSP-**1**, 68% for CSP-**2**, and 723% for CSP-**3**, showing an increasing trend. Meanwhile, the toughness of CSP-**3** (47 MJ/m^3) was also much higher than those of CSP-**1** (0.56 MJ/m^3) and CSP-**2** (9.7 MJ/m^3). These results demonstrated that the ratios of SP played a crucial role in determining the mechanical properties of the synergistic CSPs. Overall, CSP-**3** has a more balanced performance, and thus was selected as a representative of CSPs in the following research.

The mechanical properties of the three kinds of polymers were well reflected by the stress-strain curves (Figure 2d). Before linked by SP, the CP-**3** was highly stretchable (> 2000%), but possessed poor stiffness (Young's modulus = 0.15 MPa) and strength (maximum stress = 0.063 MPa). In contrast, SP was a stiff (Young's modulus = 68 MPa) but brittle material which can only be stretched to about 3% of its original length, and thus had inferior toughness (5.2 × 10^{-3} MJ/m^3). The synergistic CSP-**3** exhibited an overall improvement of mechanical properties including the aspects of stiffness (Young's modulus = 92 MPa), strength (maximum stress = 11 MPa), stretchability (723%), and toughness (47 MJ/m^3), which were clearly displayed by the radar chart (Figure 2f). Notably, the quantified values of these properties for CSP-**3** are much higher than the sum of the corresponding

10.1002/anie.202004152

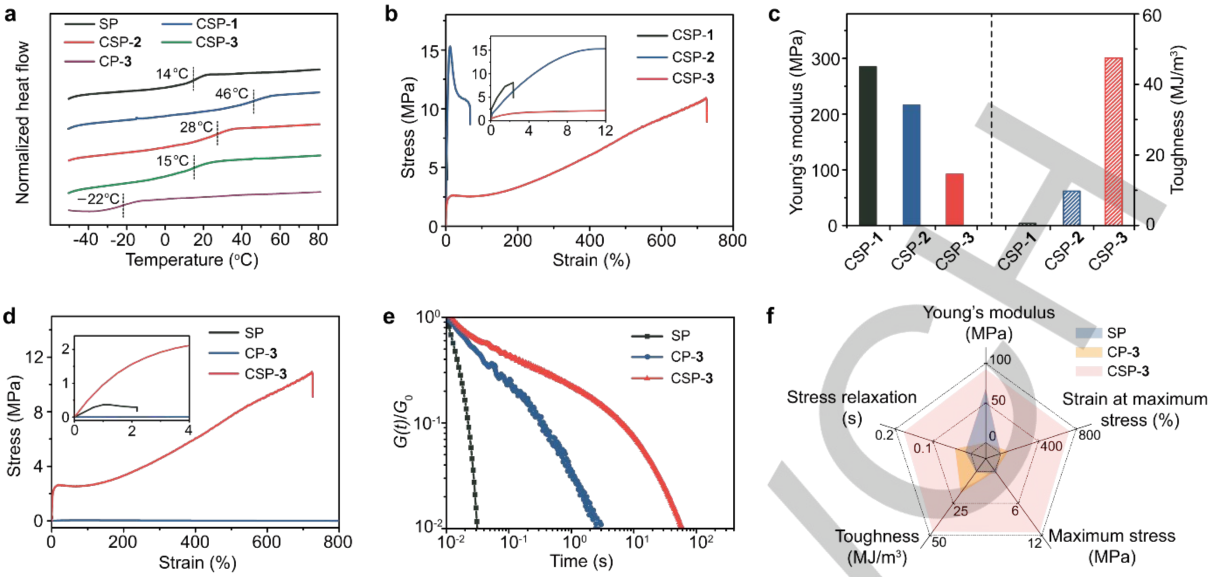

Figure 2. a) DSC curves of SP, CP-**3**, and CSPs-**1**–**3** recorded by the second heating scan from –50 to 80 °C with a heating rate of 20 °C/min. b) Stress-strain curves of CSPs-**1**–**3** recorded at room temperature with a deformation rate of 100 mm/min. c) Young's moduli and toughness of CSPs-**1**–**3** calculated based on their stress-strain curves. d) Stress-strain curves of SP, CP-**3**, and CSP-**3** recorded at room temperature with a deformation rate of 100 mm/min. e) Normalized stress-relaxation curves of SP, CP-**3**, and CSP-**3** measured at 60 °C. f) Comparison of mechanical properties and stress-relaxation time of CSP-**3** with those of SP and CP-**3**.

data for CP-**3** and SP, implying that synergistic effect is involved in the mechanical behaviors of CSP-**3**. As mentioned in the introduction part, SPs suffer from poor mechanical robustness, which is the fatal defect for their practical applications. The results in this work indicated that the combination of CPs and SPs to construct synergistic CSPs is an efficient means to improve the mechanical properties of SPs. In addition, the stress-relaxation behaviors of the three polymers were also investigated. As shown in Figure 2e, the CSP-**3** released stress much slower than individual CP-**3** or SP, and the corresponding characteristic relaxation time (1/e) was also included in the radar chart (Figure 2f). The slower stress relaxation of CSP-**3** can be attributed to that the network structure formed by CP-**3** and SP could restrict the movements of polymer chains, and the dissipation of strain energy may mainly rely on the dissociation/reassociation of host–guest interactions.

Insights into the mechanical performance of CSP-3. What are the roles of CP and SP in the mechanical behaviors of CSP-**3**? And how they realize their synergies? To clarify these issues, a series of rheology and cyclic tensile loading measurements were carried out. We firstly performed the cyclic temperature ramp tests of CSP-**3** (Figure 3a). When temperature ramped down from 120 to 40 °C, both G' and G'' increased substantially. During this process, a crossover temperature (T_c) appeared at around 79 °C. At high temperature ($T > T_c$), G'' was larger than G', indicative of the break of the network structures owing to the dissociation of host–guest interactions in SP. Upon reducing temperature, the network structures restored with $G' > G''$ at the region of $T < T_c$. Besides, the temperature ramped up process exhibited opposite viscoelastic transition. The ramp curves roughly overlapped with each other, showing relatively good thermo-reversible performance.

To discriminate the dynamic behaviors of CSP-**3** at different timescales, master curves were obtained at the reference temperature of 40 °C using the time-temperature superposition (TTS) principle, which can be divided into four different regions (Figure 3b). The region above f_g was assigned as the glassy regime where the network was frozen and chain movements were restricted. Below the frequency of f_g, the frequency region ($f_d < f < f_g$) is called the dissipative regime where G' and G'' have similar magnitude. The dissipative relaxation was caused by the relaxation of network strands between the connections of CP and SP, and was governed by the T_g.[11] In the intermediate frequency range ($f_s < f < f_d$), a pronounced plateau where the material exhibited predominately elastic property was observed. Two possible elements could be responsible for the elastic plateau, which are crosslinks and entanglements. Based on the theory, the plateau modulus (G_N) can be applied to calculate the molecular weight between two effective interactions (M_e) using the equation of $G_N = \rho RT/M_e$.[12] If we assume that the modulus fully results from the chain entanglements of CSP-**3**, the calculated value of M_e, namely, the molecular weight between two entanglement points, is about 64 kDa. This value is close to the molecular weight of the CSP-**3**, indicating that the chain entanglements are negligible in CSP-**3**. Thus, the elastic properties of CSP-**3** are mainly dominated by the network formed by CP and SP. Finally, the terminal regime of the master curve ($f < f_s$) is the viscous flow regime. In general, polymers possessing true terminal relaxation show the slope of G' and G'' with values of 2 and 1, respectively, which fits the Maxwell model. These values of CSP-**3** are lower than 2 and 1, which can be interpreted that the chain dynamics are affected by the secondary interactions, that is, the recurring dissociation/reassociation of the host–guest interactions.

Then, we proceeded to study the relationships between the synergistic effect and mechanical behaviors of the CSP-**3**. In the stretching-speed-dependent tensile tests, both Young's modulus and strength of CSP-**3** increased along with the deformation rates from 1 to 1000 mm/min (Figure S34). It is well known that the mechanical strength of polymer network with dynamic crosslinks is highly dependent on deformation rates.[13] Therefore, these

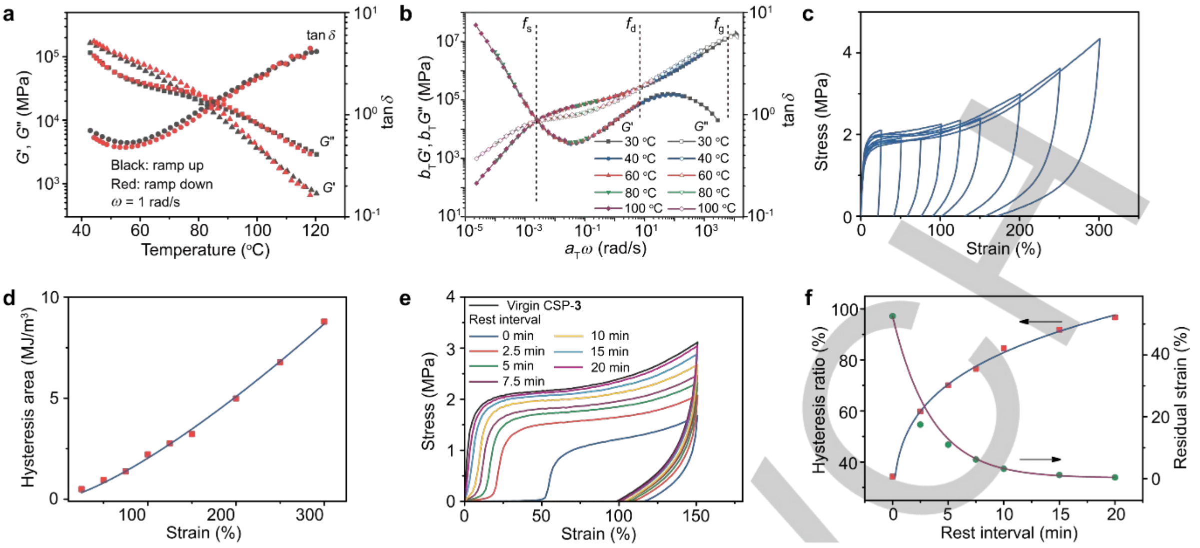

Figure 3. a) Cyclic temperature ramp curves range from 45 to 120 °C with a heating/cooling rate of 2 °C/min. b) Master curves of CSP-**3** at a reference temperature of 40 °C. c) Cyclic tensile test curves of CSP-**3** recorded at room temperature with increased maximum strains. d) Hysteresis area for each circle of cyclic tensile test curves. e) Cyclic tensile test curves of CSP-**3** loaded at a strain of 150% with rest intervals ranging from 0 to 20 min for recovery property study. The tests were performed at room temperature with a deformation rate of 100 mm/min. f) Hysteresis ratio and residual strain for each circle of cyclic tensile test curves.

results revealed that the dynamic characteristics of CSP-**3** may largely originate from the SP part. The role of SP was further disclosed by cyclic tensile tests in a broad range of maximum applied strains from 25 to 300% (Figure 3c). After reloading, CSP-**3** exhibited pronounced hysteresis and notable residual strain which increased substantially with enlarged strains. The hysteresis areas of each loading and unloading cycle were summarized in Figure 3d. These results further verified the important role of SP in energy dissipation in which the host–guest recognition acted as the sacrificial bond and dissipated the energy through its rupture.

The role of CP and its interplay with SP were demonstrated by the recovery properties of CSP-**3**. During the cyclic tensile tests, CSP-**3** was repeatedly loaded to a 150% strain and unloaded with different rest intervals ranging from 0 to 20 min. As shown in Figure 3e, the virgin circle of CSP-**3** had a plump curve due to the energy dissipation of SP. The second circle without relaxing exhibited a very small hysteresis loop because most of the dissociated host–guest interactions were not recovered. Meanwhile, the unrecovered deformation of the polymer network also led to a large residual strain of about 53%. Along with extending rest time, the host–guest recognition and the polymer network gradually recovered, and basically finished in 20 min. Thus, CSP-**3** displayed good recovery property. It is well known that during the recovery process, there is a competition between the elasticity of the polymeric system and the strength of the temporarily reformed host–guest interactions. The reformed host–guest interactions could slow down the recovery of the primary chain to its equilibrium state.[14] In CSP-**3**, the elasticity was mainly contributed by the covalent chains and the unbroken part of the network. As shown in Figure 3f, the recovery of residual strain for the sample was much faster than the recovery of hysteresis area. Because of the relatively slow reassociation of host–guest recognition, it is reasonable to deduce that compared with the hindrance from the reformed host–guest recognition, the elasticity offered by the CP and unbroken network is dominant during the recovery process, thus leading to the fast deformation recovery. Moreover, the fast recovery of deformation is beneficial to the recovery of the whole mechanical properties.

Now, the roles of SP and CP and their synergistic effect in the mechanical behaviors of CSP-**3** have been elucidated. Separately, SP could reversibly dissociate and reassociate to dissipate the energy, which is crucial to the mechanical properties such as stiffness and toughness. CP serves as the skeleton of the CSP-**3** network, and maintains the integrity of the material at a large deformation. Synergistically, these merits of SP and CP work with each other in CSP-**3** to endow it not only outstanding mechanical performance in stiffness, strength, stretchability, toughness, *etc.*, but also notable recovery property. The rheological analysis has revealed that chain entanglements are negligible in CSP-**3**, hence the mechanical properties mainly originate from the synergistic interactions of SP and CP in the network. Therefore, we can conclude that the rationally designed CSPs are able to utilize the advantages of SP and CP synergistically to produce a particular property, thereby achieving a result that one plus one is greater than two. Next, we wonder whether the innate dynamic properties of SP still retain in CSP-**3**.

Dynamic properties of CSP-3. Self-healing is highly dependent on the dynamic properties of materials and also an important indicator of dynamic properties. Here, the bulk self-healing of CSP-**3** was studied at 50 °C, and was detected by tensile tests. With the extension of healing time, the overall mechanical properties of the rejoined films including Young's modulus, tensile strength and strain, and toughness gradually restored (Figures 4a and S35). The healing efficiency evaluated by the strain at break of the restored films compared with that of the uncut one, was up to 93% after 24 h (Figure S35a), showing notable healing property.

As we know, the host–guest recognition between B21C7 and secondary ammonium salt is sensitive to pH changes through the reversible deprotonation and protonation of secondary ammonium salt. Here, triethylamine (TEA) and trifluoroacetic acid (TFA) were employed as the acid/base pair to study the pH-responsiveness of CSP-**3**. As shown in Figure 4b, When treated

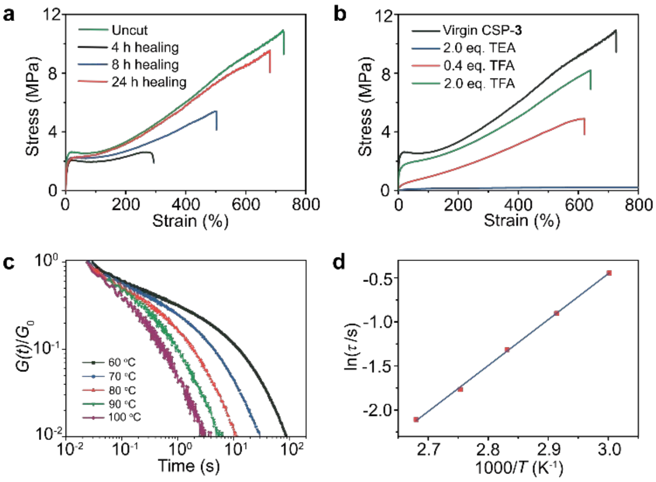

Figure 4. a) Stress-strain curves of the virgin and healed CSP-**3** specimens after three different healing times from 4 to 8 and then to 24 h at 50 °C. b) Stress-strain curves of the virgin CSP-**3** sample and those after being treated by acid/base pair of TFA and TEA. c) Normalized stress-relaxation curves of CSP-**3** at different temperatures. d) Fitting of the relaxation times to the Arrhenius equation.

by 2 equiv. of TEA, both the stiffness (Young's modulus = 0.52 MPa) and strength (maximum stress = 0.21 MPa) of the sample were poor but its stretchability was good (> 2000%), which is highly similar to the case of CP-**3**. The reason for this observation is that the TEA broke the host–guest recognition of SP, converting CSP-**3** into linear covalent polymer like CP-**3**. The broken SP could be recovered by protonation of TFA, and the degree of the recovered mechanical properties can be tuned through gradual addition of TFA. As indicated by the stress-strain curves, addition of 0.4 equiv. of TFA partially recovered the mechanical properties of the sample. Further, increasing the dosage of TFA to 2 equiv., the mechanical properties recovered mostly (Figure S37). The difference between the virgin curve and acid/base-treated one is reasonable on account of the changed microenvironment of the sample. The pH-responsiveness of CSP-**3** can also be proved by ^{1}H NMR spectra (Figure S38). Besides, CSP-**3** also exhibited obvious ion-responsiveness (Figure S39). When the PF_6^- counter anion was changed into Cl^- which doesn't favor the recognition of B21C7 to secondary ammonium salt, the mechanical properties of CSP-**3** decreased largely. Meanwhile, the mechanical properties basically recovered by exchanging the counter anion back to PF_6^-. These results suggested that the dynamic properties of SP are well retained in CSPs, and the mechanical properties of CSPs are tunable by the changes of external environments.

Furthermore, we envisioned that the dynamic properties arising from SP could also allow for reprocessing of the synergistic CSPs. To clarify this, the CSP-**3** sample was cut into small pieces and then hot pressed at 60 °C, which reformed coherent and smooth samples with different shapes (Figure S40). Impressively, the stress-strain curves of the remolded samples only changed slightly after three circles (Figure S41). These results indicated that the synergistic CSP-**3** has good malleability.

To get a deep insight into the dynamic properties of CSP-**3**, stress relaxation experiments were performed at different temperatures. As expected, the material relaxed stress faster at higher temperatures (Figure 4c). It is well known that if the stress relaxation occurs via the dissociation/reassociation of the host–guest complex, the characteristic relaxation time versus temperature should follow Arrhenius law. As shown in Figure 4d, the strict linear correlation of $\ln(\tau)$ and $1000/T$ indicates that the host–guest interactions are responsible for the stress relaxation. The activation energy of the relaxation process was calculated to be 43.3 kJ/mol, which is associated with the dissociation barrier of the B21C7/secondary ammonium salt recognition. Compared with the materials cross-linked by ureidopyrimidinone (UPy) groups or coordination bonds,[15] the activation energy of the host–guest recognition is lower. It is therefore that the host–guest complexation can work more sensitively both in the mechanical behaviors and dynamic responsivenesses.

Conclusion

In summary, we have designed and prepared three synergistic CSPs through successive ROMP of norbornene moieties and supramolecular polymerization driven by the host–guest recognition between B21C7 and secondary ammonium salt. Due to the synergistic effect, CSP-**3** exhibited notable mechanical properties in terms of stiffness (Young's modulus = 92 MPa), strength (maximum stress = 11 MPa), stretchability (723%), toughness (47 MJ/m^3), and elastic recovery (20 min), which achieve a result that one plus one is greater than two. In addition, these mechanical properties of the synergistic CSPs can be tuned by controlling the ratios of SPs and CPs. The structural basis to realize the synergistic effect and improve the mechanical properties, is the unique 3D network formed by the combination of SPs and CPs. Particularly, the rheological results have suggested that the CSP-**3** has almost pure cross-linked structure with negligible chain entanglements. Notably, in addition to originating from the synergistic interactions, the properties of CSP-**3** also inherit from the innate properties of SP and CP, such as the well preserved self-healing, stimuli-responsive, and reprocessing properties of SP in CSP-**3**. Therefore, the CSP-**3** could possess not only good mechanical performance but also multiple dynamic properties. As far as we know, this work represents the first artificial elastomeric materials of synergistic CSPs. To further develop the concept, constructing synergistic CSPs with various well-designed structures, enriching and enhancing their properties and functions, and exploiting their potentials in specific applications are being actively pursued in our lab.

Acknowledgements

X.Y. acknowledges the financial support of the NSFC/China (21901161), Program for Eastern Scholar of Shanghai, and start-up funds from Shanghai Jiao Tong University. W.Y. acknowledges the financial support of the NSFC/China (51625303).

Keywords: supramolecular polymers • host–guest chemistry • synergistic effect • mechanically adaptive properties • dynamic materials

[1] a) A. M. Gordon, E. Homsher, M. Regnier, *Physiol. Rev.* **2000**, *80*, 853–924; b) L. R. Otterbein, P. Graceffa, R. Dominguez, *Science* **2001**, *293*, 708–711; c) B. Barua, D. A. Winkelmann, H. D. White, S. E. Hitchcock-DeGregori, *Proc. Natl. Acad. Sci. USA* **2012**, *109*,

18425–18430; d) J. Von der Ecken, M. Müller, W. Lehman, D. J. Manstein, P. A. Penczek, S. Raunser, *Nature* **2015**, *519*, 114–117.

[2] a) L. Montero de Espinosa, W. Meesorn, D. Moatsou, C. Weder, *Chem. Rev.* **2017**, *117*, 12851–12892; b) S. Erbas-Cakmak, S. D. Fielden, U. Karaca, D. A. Leigh, C. T. McTernan, D. J. Tetlow, M. R. Wilson, *Science* **2017**, *358*, 340–343; c) R. Baumgartner, H. Fu, Z. Song, Y. Lin, J. Cheng, *Nat. Chem.* **2017**, *9*, 614–622; d) J. Chen, F. K. C. Leung, M. C. Stuart, T. Kajitani, T. Fukushima, E. van der Giessen, B. L. Feringa, *Nat. Chem.* **2018**, *10*, 132–138.

[3] Z. Yu, F. Tantakitti, T. Yu, L. C. Palmer, G. C. Schatz, S. I. Stupp, *Science* **2016**, *351*, 497–502.

[4] X. Hou, C. Ke, Y. Zhou, Z. Xie, A. Alngadh, D. T. Keane, M. S. Nassar, Y. Y. Botros, C. A. Mirkin, J. F. Stoddart, *Chem. Eur. J.* **2016**, *22*, 12301–12306.

[5] a) L. Brunsveld, B. J. B. Folmer, E. W. Meijer, R. P. Sijbesma, *Chem. Rev.* **2001**, *101*, 4071–4098; b) X. Yan, F. Wang, B. Zheng, F. Huang, *Chem. Soc. Rev.* **2012**, *41*, 6042–6065; c) Y. Chen, A. M. Kushner, G. A. Williams, Z. Guan, *Nat. Chem.* **2012**, *4*, 467–472; d) T. Aida, E. W. Meijer, S. I. Stupp, *Science* **2012**, *335*, 813–817; e) L. Yang, X. Tan, Z. Wang, X. Zhang, *Chem. Rev.* **2015**, *115*, 7196–7239; f) E. Krieg, M. M. C. Bastings, P. Besenius, B. Rybtchinski, *Chem. Rev.* **2016**, *116*, 2414–2477; g) S. Dong, J. Leng, Y. Feng, M. Liu, C. J. Stackhouse, A. Schönhals, L. Chiappisi, L. Gao, W. Chen, J. Shang, L. Jin, Z. Qi, C. A. Schalley, *Sci. Adv.* **2017**, *3*, eaao0900; h) H. Chen, Z. Huang, H. Wu, J.-F. Xu, X. Zhang, *Angew. Chem. Int. Ed.* **2017**, *56*, 16575–16578; *Angew. Chem.* **2017**, *129*, 16802–16805; i) S. Wang, J. Xu, W. Wang, G.-J. N. Wang, R. Rastak, F. Molina-Lopez, J. W. Chung, S. Niu, V. R. Feig, J. Lopez, T. Lei, S.-K. Kwon, Y. Kim, A. M. Foudeh, A. Ehrlich, A. Gasperini, Y. Yun, B. Murmann, J. B.-H. Tok, Z. Bao, *Nature* **2018**, *555*, 83–88; j) T. L. Price Jr, H. W. Gibson, *J. Am. Chem. Soc.* **2018**, *140*, 4455–4465; k) Y. Han, Y. Tian, Z. Li, F. Wang, *Chem. Soc. Rev.* **2018**, *47*, 5165–5176; l) X. Tang, Z. Huang, H. Chen, Y. Kang, J.-F. Xu, X. Zhang, *Angew. Chem. Int. Ed.* **2018**, *57*, 8545–8549; *Angew. Chem.* **2018**, *130*, 8681–8685; m) X. Zhang, L.-Y. Wang, J.-F. Xu, D.-Y. Chen, L.-Q. Shi, Y.-F. Zhou, Z.-H. Shen, *Acta Polym. Sin.* **2019**, *50*, 973–987; n) K. Liu, Y. Jiang, Z. Bao, X. Yan, *CCS Chem.* **2019**, *1*, 431–447.

[6] a) G. Sun, S. Cho, C. Clark, S. V. Verkhoturov, M. J. Eller, A. Li, A. Pavía-Jiménez, E. A. Schweikert, J. W. Thackeray, P. Trefonas, K. L. Wooley, *J. Am. Chem. Soc.* **2013**, *135*, 4203–4206; b) A. B. Chang, T. P. Lin, N. B. Thompson, S. X. Luo, A. L. Liberman-Martin, H. Y. Chen, B. Lee, R. H. Grubbs, *J. Am. Chem. Soc.* **2017**, *139*, 17683–17693; c) P. Shieh, H. V. T. Nguyen, J. A. Johnson, *Nat. Chem.* **2019**, *11*, 1124–1132.

[7] a) C. Zhang, S. Li, J. Zhang, K. Zhu, N. Li, F. Huang, *Org. Lett.* **2007**, *9*, 5553–5556; b) Z.-J. Zhang, H.-Y. Zhang, H. Wang, Y. Liu, *Angew. Chem. Int. Ed.* **2011**, *50*, 10834–10838; *Angew. Chem.* **2011**, *123*, 11026–11030; c) L. Wang, L. Cheng, G. Li, K. Liu, Z. Zhang, P. Li, S. Dong, W. Yu, F. Huang, X. Yan, *J. Am. Chem. Soc.* **2020**, *142*, 2051–2058.

[8] a) D. Mozhdehi, S. Ayala, O. R. Cromwell, Z. Guan, *J. Am. Chem. Soc.* **2014**, *136*, 16128–16131; b) M. Arunachalam, H. W. Gibson, *Prog. Polym. Sci.* **2014**, *39*, 1043–1073; c) C.-H. Li, C. Wang, C. Keplinger, J.-L. Zuo, L. Jin, Y. Sun, P. Zheng, Y. Cao, F. Lissel, C. Linder, X.-Z. You, Z. Bao, *Nat. Chem.* **2016**, *8*, 618–624; d) S. Yoshida, H. Ejima, N. Yoshie, *Adv. Funct. Mater.* **2017**, *27*, 1701670; e) X. Yan, Z. Liu, Q. Zhang, J. Lopez, H. Wang, H.-C. Wu, S. Niu, H. Yan, S. Wang, T. Lei, J. Li, D. Qi, P. Huang, J. Huang, Y. Zhang, Y. Wang, G. Li, J. B.-H. Tok, X. Chen, Z. Bao, *J. Am. Chem. Soc.* **2018**, *140*, 5280–5289; f) S. Wang, Z. Xu, T. Wang, T. Xiao, X.-Y. Hu, Y.-Z. Shen, L. Wang, *Nat. Commun.* **2018**, *9*, 1737; g) Y. Song, Y. Liu, T. Qi, G. L. Li, *Angew. Chem. Int. Ed.* **2018**, *57*, 13838–13842; *Angew. Chem.* **2018**, *130*, 14034–14038; h) Z. Wang, Y. Ren, Y. Zhu, L. Hao, Y. Chen, G. An, H. Wu, X. Shi, C. Mao, *Angew. Chem. Int. Ed.* **2018**, *57*, 9008–9012; *Angew. Chem.* **2018**, *130*, 9146–9150.

[9] a) C. W. Bielawski, D. Benitez, T. Morita, R. H. Grubbs, *Macromolecules* **2001**, *34*, 8610–8618; b) M. Liu, J. van Hensbergen, R. P. Burford, A. B. Lowe, *Polym. Chem.* **2012**, *3*, 1647–1658.

[10] E. S. Stoyanov, C. A. Reed, *J. Phys. Chem. A* **2004**, *108*, 907–913.

[11] J. C. Majeste, J. P. Montfort, A. Allal, G. Marin, *Rheologica acta* **1998**, *37*, 486–499.

[12] A. Susa, R. K. Bose, A. M. Grande, S. Van Der Zwaag, S. J. Garcia, *ACS Appl. Mater. Interfaces* **2016**, *8*, 34068–34079.

[13] a) T. L. Sun, T. Kurokawa, S. Kuroda, A. B. Ihsan, T. Akasaki, K. Sato, M. A. Haque, T. Nakajima, J. P. Gong, *Nat. Mater.* **2013**, *12*, 932–937; b) D. G. Mackanic, X. Yan, Q. Zhang, N. Matsuhisa, Z. Yu, Y. Jiang, T. Manika, J. Lopez, H. Yan, K. Liu, X. Chen, Y. Cui, Z. Bao, *Nat. Commun.* **2019**, *10*, 5384.

[14] J. Liu, J. Liu, S. Wang, J. Huang, S. Wu, Z. Tang, B. Guo, L. Zhang, *J. Mater. Chem. A* **2017**, *5*, 25660–25671.

[15] a) L. Yang, G. Zhang, N. Zheng, Q. Zhao, T. Xie, *Angew. Chem. Int. Ed.* **2017**, *56*, 12599–12602; *Angew. Chem.* **2020**, *129*, 12773–12776; b) Y. Meng, W. Xu, M. R. Newman, D. S. Benoit, M. Anthamatten, *Adv. Funct. Mater.* **2019**, *29*, 1903721.

Entry for the Table of Contents

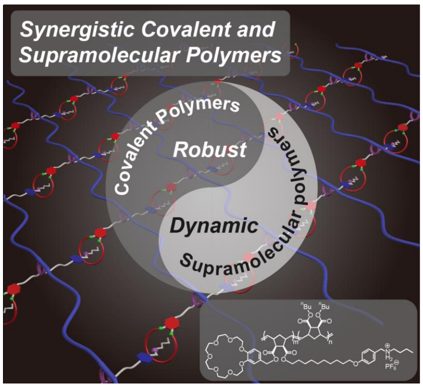

Inspired by bio-system, synergistic covalent and supramolecular polymers (CSPs) are developed for the construction of mechanically robust yet dynamic materials. They are able to integrate and even enhance the merits of covalent polymers and supramolecular polymers, and achieve a result that one plus one is greater than two.